Sources and oxidative potential of water-soluble humic-like substances ($HULIS_{WS}$) in fine particulate matter ($PM_{2.5}$) in Beijing

Yiqiu Ma[1,2], Yubo Cheng[2], Xinghua Qiu*[,1], Gang Cao[3], Yanhua Fang[1], Junxia Wang[1], Tong Zhu[1], Jianzhen Yu[4], Di Hu*[,2,5,6]

[1]State Key Joint Laboratory for Environmental Simulation and Pollution Control, College of Environmental Sciences and Engineering, Peking University, Beijing 100871, P. R. China
[2]Department of Chemistry, Hong Kong Baptist University, Kowloon Tong, Kowloon, Hong Kong, P. R. China
[3]School of Civil and Environment Engineering, Harbin Institute of Technology Shenzhen Graduate School, Shenzhen, 518057, P.R. China
[4]Department of Chemistry, Hong Kong University of Science and Technology, Clear Water Bay, Kowloon, Hong Kong, P. R. China
[5]State Key Laboratory of Environmental and Biological Analysis, Hong Kong Baptist University, Kowloon Tong, Kowloon, Hong Kong, P. R. China
[6]HKBU Institute of Research and Continuing Education, Shenzhen Virtual University Park, Shenzhen, 518057, P. R. China

Correspondence to: Xinghua Qiu (xhqiu@pku.edu.cn); Di Hu (dihu@hkbu.edu.hk)

Abstract. Water-soluble humic-like substances ($HULIS_{WS}$) are a major redox-active component of ambient fine particulate matter ($PM_{2.5}$); however, information on their sources and associated redox activity is limited. In this study, $HULIS_{WS}$ mass concentration, various $HULIS_{WS}$ species, and dithiothreitol (DTT) activity of $HULIS_{WS}$ were quantified in $PM_{2.5}$ samples collected during a 1-year period in Beijing. Strong correlation was observed between $HULIS_{WS}$ and DTT activity; both exhibited higher levels during the heating season than during the non-heating season. Positive matrix factorization analysis of both $HULIS_{WS}$ and DTT activity was performed. Four combustion-related sources, namely coal combustion, biomass burning, waste incineration, and vehicle exhaust, and one secondary factor were resolved. In particular, waste incineration was identified as a source of $HULIS_{WS}$ for the first time. Biomass burning and secondary aerosol formation were the major contributors (>59%) to both $HULIS_{WS}$ and associated DTT activity throughout the year. During the non-heating season, secondary aerosol formation was the most important source, whereas during the heating season, the predominant contributor was biomass burning. The four combustion-related sources accounted for >70% of $HULIS_{WS}$ and DTT activity, implying that future reduction in $PM_{2.5}$ emissions from combustion activities can substantially reduce the $HULIS_{WS}$ burden and their potential health impact in Beijing.

1 Introduction

Fine particulate matter ($PM_{2.5}$) pollution has caused both environmental and public health problems worldwide. $PM_{2.5}$ can travel deep into the human lung and lead to various respiratory diseases, such as respiratory tract infections, chronic cough, and asthma (Becker et al., 2005; Nel, 2005). Given the various sources and complex chemical composition of $PM_{2.5}$, the underlying mechanisms of $PM_{2.5}$ exposure-induced adverse health effects are not fully understood yet. However, it has been postulated that, the redox-active components on $PM_{2.5}$, such as transition metals and quinones (Charrier and Anastasio, 2012; Chung et al., 2006), can perturb the redox equilibrium in lung cell through the generation of excessive reactive oxygen species (ROS), and induce the subsequent oxidative stress.

Humic-like substances ($HULIS_{WS}$) are a mixture of compounds containing polycyclic ring structures with aliphatic side chains and multiple polar functional groups. They account for a significant proportion (30%–80%) of the water-soluble organic matter (WSOM) in $PM_{2.5}$ (Graber and Rudich, 2006; Kuang et al., 2015; Lin et al., 2010a). $HULIS_{WS}$ have recently been recognized to

be highly redox-active and they play a significant role in driving PM-associated ROS formation (Dou et al., 2015; Lin and Yu, 2011; Verma et al., 2015a). The reversible redox sites in $HULIS_{WS}$ fraction could serve as an electron transfer intermediate and lead to continuous production of ROS (Lin and Yu, 2011). Dithiothreitol (DTT) assay have been widely used to evaluate the oxidative capacity of $HULIS_{WS}$ and $PM_{2.5}$. Verma et al. (2015b) found that $HULIS_{WS}$ contributed approximately 45% of DTT activity of the water extracts from $PM_{2.5}$ samples collected in Atlanta, USA, which was 5% higher than that induced by water-soluble metals. Lin and Yu (2011) also found that $HULIS_{WS}$ accounted for 79%±12% of DTT activity caused by WSOM fraction in $PM_{2.5}$ sampled in Pearl River Delta (PRD) region, China. Given the considerable amount of $HULIS_{WS}$ in $PM_{2.5}$ and their ROS generation ability, both field measurements and smog chamber experiments have been conducted to determine their formation pathways and origins in the atmosphere (Kautzman et al., 2010; Lin et al., 2010b; Sato et al., 2012). Biomass burning and secondary formation have been suggested to be the major sources of atmospheric $HULIS_{WS}$ (Kautzman et al., 2010; Lin et al., 2010b). However, studies on the quantitative source apportionment of $HULIS_{WS}$ are still limited (Kuang et al., 2015), and information on the source-specific contribution to their redox activity is lacking.

Beijing, the capital of China located in the North China Plain, is a political and cultural center with an extremely dense population. On the other hand, it has become one of the most polluted cities in the world, with an annual $PM_{2.5}$ concentration of up to 89.5 μg m^{-3} in 2013 (Li et al., 2017). Therefore, it presents an ideal location to study the chemical characteristics of $HULIS_{WS}$ as well as their sources and potential redox activity.

In this study, our major objective is to investigate the ROS-forming ability of $HULIS_{WS}$ in relation to different sources and meteorological conditions. Thus, a total of 66 $PM_{2.5}$ samples collected in Beijing during a 1-year period were analyzed. Concentrations of total $HULIS_{WS}$ were quantified, together with some characteristic individual $HULIS_{WS}$ species and the major aerosol components. The redox activity of $HULIS_{WS}$ was determined using a DTT assay. Positive matrix factorization (PMF) analysis was conducted to determine the sources of both $HULIS_{WS}$ and their associated redox activity. Such a comprehensive source apportionment study of $HULIS_{WS}$-related ROS-generation potential has not been previously reported. Results from this study could provide not only quantitative information regarding the sources and toxicity of $HULIS_{WS}$, but also a deeper understanding of the source-specific oxidative potential of Chinese urban organic aerosols in general. This may be useful for the future development of source-targeted air pollution control policies in Beijing and may provide public-health benefits.

2 Material and methods

2.1 Sample collection

$PM_{2.5}$ samples were collected at the Peking University Atmosphere Environment Monitoring Station (PKUERS) on the campus of Peking University (39°59'21"N, 116°18'25'E, approximately 30 m above the ground), Beijing, China. A high-volume air sampler coupled with a ≤2.5 μm inlet (HIVOL-CABLD, ThermoFisher Scientific, Waltham, MA, USA) was used to conduct sampling at a flow rate of 1.13 m^3 min^{-1}. Samples were collected on quartz fiber filters (20.3 × 25.4 cm^2, prebaked at 550 °C for 5 h; Whatman, Hillsboro, OR, USA) for 24 h every 6 days from 3 March 2012 to 1 March 2013. In addition, a four-channel mid-volume sampler was operated synchronously (16.7 L min^{-1}, TH-16A, Wuhan Tianhong Instruments Co. Ltd, China) to collect $PM_{2.5}$ onto three 47-mm Teflon filters and one quartz fiber filter for the determination of $PM_{2.5}$ mass, elemental carbon (EC) and organic carbon (OC), and inorganic ionic species.

2.2 Chemical analysis

$HULIS_{WS}$ was isolated from $PM_{2.5}$ samples following the procedure described by Lin et al. (2010b). Briefly, a portion of sample filters (17.5 cm^2 for $HULIS_{WS}$ species identification and 3 cm^2 for $HULIS_{WS}$ mass measurement) was cut into small pieces and pollutants were extracted through sonication with distilled deionized (DDI) water for 30 min. The extracts were filtered with polytetrafluoroethylene (PTFE) filters (0.45-μm pore size; Grace, Houston TX, USA) and acidified to a pH of 2 with 2.4 M HCl. A solid phase extraction (SPE) cartridge (Oasis HLB, 3 mL/30 μm, 60 mg; Waters, Milford, MA, USA) was used to isolate $HUILS_{WS}$. The SPE cartridge was first activated using 1.0 mL of methanol and equilibrated using 1.0 mL of 0.01 M HCl. The extracts were then loaded onto an HLB cartridge. Because the majority of inorganic ions, low molecular weight organic acids, and sugar compounds could not be retained by the HLB cartridge, they were removed from the final effluent. For the analysis of individual $HULIS_{WS}$ species, the HLB cartridge was rinsed with two 1.0-mL portions of DDI water and then eluted with three 0.5-mL portions of basic methanol (2% ammonia, w/w). The effluent was dried with a gentle flow of ultrapure nitrogen at 40 °C, and then derivatized with 100 μL of N,O-bis(trimethylsilyl)trifluoroacetamide (BSTFA; with 1% trimethylchlorosilane; Sigma Aldrich, St. Louis, MO, USA) and 50 μL of pyridine (>99.5%; International Laboratory USA, CA, USA) at 70 °C for 2 h. When the mixture had cooled to room temperature, it was spiked with 30 μL of tetracosane-d_{50} (50 μg mL^{-1} in n-hexane; Sigma Aldrich, St. Louis, MO, USA) as the internal standard for gas chromatography-mass spectrometry (GC-MS; 5975-7890A, Agilent, Santa Clara, CA, USA) analysis. Detailed information on this analysis is provided in the Supplementary Material.

For the quantification of $HULIS_{WS}$ mass concentration, 6.0 mL of pure methanol was used to elute $HULIS_{WS}$ from HLB cartridge instead of 1.5 mL of basic methanol (2% ammonia, w/w). This is to avoid possible influence of ammonia in the following DTT experiments (Lin and Yu, 2011), and larger volume of methanol was used to maintain the elution efficiency (Lin and Yu, 2011). Comparison on the GC-MS peak intensities of individual $HULS_{WS}$ species eluted by these two protocols was provided in the Supplementary Material (Figure S1). The effluent was dried with nitrogen, and restored in 1 mL of DDI water for quantification. An aliquot of 20 μL of aqueous solution was injected into a high-performance liquid chromatography system (HPLC, ThermoFisher Scientific, Waltham, MA, USA) coupled with an evaporative light scattering detector (Alltech ELSD 3300, Grace, Houston, TX, USA). Since ELSD is mass sensitive, the mass of $HULIS_{WS}$ instead of $HULIS_{WS}$_carbon was reported in this study. Detailed information on the HPLC-ELSD operation conditions is provided in the Supplementary Material.

Major water-soluble ions were identified and quantified using ion-chromatography (DIONEX, ICS-2500 for cations and ICS-2000 for anions, ThermoFisher Scientific, Waltham, MA, USA, Tang et al., 2011). EC and OC were analyzed by a thermal–optical carbon analyzer (Sunset Laboratory-Based Instrument, Tigard, OR, USA, Tang et al., 2011). Hopanes were measured by in-injection thermal desorption-gas chromatography mass spectrometry (GC-MS, Agilent 6890N-5975C, Santa Clara, CA, USA, Ho and Yu, 2004), while levoglucosan was measured using an Agilent 7890A- 5975C GC-MS (Hu et al., 2008). Concentrations of hopanes, levoglucosan, water-soluble ions, EC and OC were listed in Table S1 in the Supplementary Material.

2.3 DTT assay

We followed the procedure of Li et al. (2009) and Lin and Yu (2011) for DTT experiments. Briefly, a 120-μL portion of $HULIS_{WS}$ solution was transferred into an eppendorf tube. Then 920 μL of potassium phosphate buffer (pH = 7.4) containing 1 mM diethylene triamine pentaacetic acid (DTPA) and 50 μL of 0.5 mM DTT (both >99%; Sigma Aldrich, St. Louis, MO, USA) were added and mixed thoroughly. The samples were subsequently placed in a dry bath at 37 °C for 90 min and spiked with 100 μL of 1.0 mM 5,5'-dithiobis-2-nitrobenzoic acid (DTNB, 98%; Sigma Aldrich, USA) containing 1 mM DTPA. Considering the reaction between DTNB and DTT was very fast, the absorption could reach its maximum value immediately and stay stable for more than 2 hours (Li et al., 2009). So we followed the same protocol described in Li et al. (2009) with the elimination of quenching step described

in Cho et al.'s method (2005), and conduct measurement at 412 nm within 30 min using an ultraviolet-visible (UV-Vis) spectrophotometer (8453, Hewlett Pakard, Palo Alto, CA, USA). Considering that some transition metals may still remain in the $HULIS_{WS}$ fraction even after HLB purification, sufficient amount of DTPA was added in the procedure to chelate all the remaining transition metals, such as Cu, Mn, and Fe, to eliminate the DTT consumption by these metals (Lin and Yu, 2011). For the control samples, blank filters were used instead of real samples.

Previous study observed that the time-dependent consumption of DTT catalysed by $HULIS_{WS}$ was linear when DTT consumption was less than 90% (Lin and Yu, 2011). We have also examined the $HULIS_{WS}$-catalysed DTT consumption as a function of time and obtained a similar result as Lin and Yu (2011). In our study, the $HULIS_{WS}$-catalysed DTT consumption of all 66 samples were between 3.6% and 77.0%, and the measured DTT activity was linearly proportional to $HULIS_{WS}$ mass concentration.

The $HULIS_{WS}$-catalysed DTT consumption of each sample was normalized by the volume of air sampled (DTT_V, defined as extrinsic DTT activity and expressed in units of nmol min^{-1} m^{-3}) and the $HULIS_{WS}$ mass (DTT_m, defined as intrinsic DTT activity and expressed in units of mol min^{-1} per μg $HULIS_{WS}$) (Dou et al., 2015; Verma et al., 2014), respectively. The mathematical expressions of DTT_V and DTT_m are shown below.

$$Extrinsic\ DTT\ activity\ (DTT_V) = \frac{R_{DTT}(\%) \times n_{DTT}(nmol)}{t(min) \times Air\ volumn(m^{-3})} \quad \text{E.q. (1)}$$

$$Intrinsic\ DTT\ activity\ (DTT_m) = \frac{DTT_V\ (nmol\ \min\ m^{-3})}{HULIS_{WS}\ (\mu g\ m^{-3})} \quad \text{E.q. (2)}$$

Since DTPA was added to suppress DTT consumption by metals ions throughout the incubation process and may affect the DTT response of quinones (Dou et al., 2015), the DTT activity of $HULIS_{WS}$ measured here may be underestimated and is not directly comparable to those studies conducting DTT assay experiments without DTPA.

2.4 Source apportionment

In this study, the United States Environmental Protection Agency PMF 5.0 was applied to identify the sources of $HULIS_{WS}$ and apportion their contributions to both $HULIS_{WS}$ and the extrinsic DTT activity of $HULIS_{WS}$. As suggested by Henry et al. (1984), the minimum sample size of N for PMF analysis was 30 + (V + 3)/2, where V is the number of input species. A total of 66 samples and 13 species were included in PMF analysis, which was an adequate sample size to obtain a statistically reliable PMF result. Details of PMF parameter settings are provided in the Supplementary Material.

3 Results and discussion

3.1 $HULIS_{WS}$ mass concentration and the DTT activity of $HULIS_{WS}$

In this study, the $HULIS_{WS}$ mass concentration and DTT activity of $HULIS_{WS}$ in 66 $PM_{2.5}$ samples were quantified. The annual average concentration of total $HULIS_{WS}$ in Beijing measured in this study was 5.66 μg m^{-3} (median: 4.30, range: 1.08–22.36 μg m^{-3}). This was approximately 20% higher than those measured in three other Chinese cities: 4.83 μg m^{-3} in Guangzhou (Kuang et al., 2015), 4.71 μg m^{-3} in Nansha (Kuang et al., 2015), and 4.69 μg m^{-3} in Lanzhou (Tan et al., 2016). A clear temporal variation of $HULIS_{WS}$ mass concentration was observed (Figures 1, 2), with significantly higher levels ($p < 0.05$, Mann–Whitney test) in the heating season (November through March; average 7.93, median 6.15 μg m^{-3}) than in the non-heating season (April through October; average 3.72, median 2.86 μg m^{-3}). This could be mostly attributed to the intensive coal and biomass burning activities performed for residential heating during the heating season. In addition, the lower temperatures and mixing height during the heating season could also favour the formation of particle-bound $HULIS_{WS}$ species. However, the contributions of total $HULIS_{WS}$ to organic matter (OM, calculated by multiplying OC with 1.98 and 1.50 for the heating and non-heating seasons, respectively, Xing et al., 2013) in $PM_{2.5}$ are slightly lower during the heating season (21.8% ± 13.5%) than that during the non-heating season

(27.4% ± 12.0%, Figure 1), indicating higher levels of combustion-generated organic compounds other than $HULIS_{WS}$ were emitted in the heating seasons as well.

The extrinsic DTT activity of $HULIS_{WS}$ exhibited similar temporal variation as $HULIS_{WS}$ (Figure 2), with significantly higher levels in the heating season (average 0.073, median 0.063 nmol min^{-1} m^{-3}) than in the non-heating season (average 0.031, median 0.029 nmol min^{-1} m^{-3}). Because most of the inorganic ions were not retained by the HLB cartridge and the remaining metals in the $HULIS_{WS}$ effluent were chelated by DTPA, the DTT activity measured here could be attributed entirely to the DTT active moieties in $HULIS_{WS}$. The intrinsic DTT activity of $HULIS_{WS}$ describes the intrinsic ROS-generation ability of $HULIS_{WS}$, and the average intrinsic DTT activity of $HULIS_{WS}$ in Beijing was 9.91 pmol min^{-1} per μg $HULIS_{WS}$ (median 9.02, range 2.74–25.8 pmol min^{-1} per μg $HULIS_{WS}$), which was higher than the reported average DTT_m activity (6.4 ± 1.2 pmol min^{-1} per μg $HULIS_{WS}$) in six $PM_{2.5}$ samples collected during winter in Guangdong, China (Dou et al., 2015). This difference might be attributed to the different chemical components and sources of $HULIS_{WS}$ in these two regions.

3.2 Individual species of $HULIS_{WS}$

Because the main objective of this study was to identify the sources of $HULIS_{WS}$ and quantify the source-specific contributions to both $HULIS_{WS}$ and their associated redox activity, we mainly focused on the identification of organic markers in the chemical analysis. A total of 25 species were identified and quantified in the $HULIS_{WS}$ fraction of $PM_{2.5}$ using GC-MS, including 12 aromatic acids, five nitrophenol analogues, three aliphatic acids, and five biogenic secondary organic aerosol (SOA) tracers (Table S2 in the Supplementary Material, Hu et al., 2008)

All 12 aromatic acids, including three hydroxyl benzoic acids, three benzenedicarboxylic acids, three benzenetricarboxylic acids, 2-hydroxy-5-nitrobenzoic acid, vanillic acid, and syringic acid, exhibited higher levels during the heating season than during the non-heating season (Figure S2 in the Supplementary Material). Among these acids, terephthalic acid (TPha) was the most abundant (average 150.2 ng m^{-3} in the heating season, and 98.1 ng m^{-3} in the non-heating season), accounting for approximately 2% of the $HULIS_{WS}$ mass concentration. Compared with other Chinese cities, the concentration of TPha in Beijing was substantially higher than those in the southern cities, such as Hong Kong (19.9 ng m^{-3} in winter, Ho et al., 2011), and was similar to those in the northern cities, such as Xi'an (54 ng m^{-3} in summer and 250 ng m^{-3} in winter, Cheng et al., 2013). TPha is mainly used to produce polyethyleneterephthalate (PET) plastics, which are widely used for bottles and containers; therefore, it has been suggested as a tracer for the pyrolysis of domestic waste (Kawamura and Pavuluri, 2010; Simoneit et al., 2005). Benzenetricarboxylic acids were considered to be secondarily formed from the photodegradation of organic precursors, such as polycyclic aromatic hydrocarbons (PAHs) (Kautzman et al., 2010). Therefore, 1,2,3-benzenetricarboxylic acid (123Ben) and 1,2,4-benzenetricarboxylic acid (124Ben) were also included in the PMF analysis.

Similar to the aromatic acids, all five nitrophenol analogues, namely 4-nitrophenol, 2-nitrocatechol, 2-methyl-4-nitrophenol (2M4NP), 4-methly-5-nitrocatechol (4M5NC), and 3-methly-6-nitrocatechol (3M6NC), exhibited 8–14 times higher concentrations during the heating season than during the non-heating season (Table S1 in the Supplementary Material). In particular, 4M5NC and 3M6NC not only showed similar temporal variations but also were strongly correlated ($R^2 = 0.87$), implying that they may have similar sources. These two compounds have been suggested as tracers for the aging process of biomass burning (Iinuma et al., 2010; Kahnt et al., 2013). However, Iinuma et al. (2010) pointed out that the photo-oxidation of vehicle exhaust may be a more significant source for these two compounds in urban areas. Given that both 4M5NC and 3M6NC are good anthropogenic SOA markers, they were also included in the PMF analysis.

Five biogenic SOA tracers including 3-hydroxyglutaric acid, 3-hydroxy-4,4-dimethylglutaric acid, 3-methyl-1,2,3-butanetricarboxylic acid, 3-isopropylglutaric acid, and 3-acetylglutaric acid were identified and quantified. Because they were all formed from the atmospheric oxidation of monoterpenes and had similar temporal variations, they were grouped as SOA markers of monoterpenes (MonoT) in the PMF analysis (Hu et al., 2010). Briefly, MonoT showed higher concentrations during the non-heating season (average 16.9, median 15.2 ng m^{-3}) than during the heating season (average 12.5, median 10.2 ng m^{-3}), which was opposite to $HULIS_{WS}$ mass concentration. Because of the higher biogenic volatile organic compounds (VOCs) emissions, more intense solar radiation, and higher temperature and humidity in the non-heating season, more active secondary formation could lead to higher concentrations of biogenic SOA (Guo et al., 2012).

3.3 Source apportionment of $HULIS_{WS}$ and their extrinsic DTT activity

The optimal PMF solution was determined with five factors (A–E; Figure 3). The Q_{robust} obtained was 62.9, which was exactly equal to Q_{true}, and the scaled residues for all species were between −2 and +2, indicating no outliers for this solution. Constrained model operation was adopted for a more reasonable interpretation ($dQ_{robust}\% = 0.32\%$) (Norris et al., 2014). The optimized solution was bootstrapped 100 times, with 100% of the runs producing the same factors. A strong linear correlation between the measured and PMF-predicted $HULIS_{WS}$ mass concentrations ($R^2 = 0.76$) also suggested a reliable PMF solution (Figure S4 in the Supplementary Material).

As shown in Figure 3, factor A had a high percentage of non-sea salt Cl^- (nss-Cl^-, [nss-Cl^-] = [Cl^-] − 1.17 × [Na^+]), and was attributed to coal combustion (Tan et al., 2016; Tao et al., 2016; Zhang et al., 2013). Factor B had a high loading of levoglucosan and was determined as biomass burning (Hu et al., 2010; Tao et al., 2016). Factor C was considered to be waste incineration, due to the high level of TPha. Factor D was dominated by hopanes, tracers for fuel combustion, suggesting traffic related activities (Hu et al., 2010). In particular, the two anthropogenic SOA markers, 4M5NC and 3M6NC, were mostly assigned to this factor (4M5NC 46%, and 3M6NC 33%) instead of factor C (4M5NC 14%, and 3M6NC 25%). These two species were mainly formed through the photo-oxidation of cresols, which were directly emitted through wood combustion or produced from toluene through its reaction with OH radicals in the presence of NO_X (Iinuma et al., 2010). Traffic emissions were a significant source of single-ring aromatics, especially toluene, in Chinese megacities (Huang et al., 2015). In this study, the sampling site was located in an urban area influenced by considerable vehicular emissions of NO_X and toluene, which may have led to subsequent secondary formation of 4M5NC and 3M6NC. Therefore, the fourth factor was considered as a mixed source including both primary emission and the aging process of traffic exhaust. The fifth factor was characterized by a predominant loading of MonoT, SO_4^{2-}, and NH_4^+; thus, it was considered as a secondary aerosol formation source.

3.4 Source-specific contributions to $HULIS_{WS}$

Source-specific contributions to $HULIS_{WS}$ during both non-heating and heating seasons were calculated based on PMF results. The four combustion-related sources contributed >80% of $HULIS_{WS}$ in the heating season and 50% in the non-heating season (Figure 4A), of which biomass burning was the most predominant. A strong correlation ($R^2 = 0.51$, Figure S5 in the Supplementary Material) was observed between $HULIS_{WS}$ and levoglucosan, a marker of biomass burning, and this was consistent with previous studies (Lin et al., 2010b). Approximately 33% of $HULIS_{WS}$ was attributed to biomass burning during the 1-year sampling period in Beijing, higher than that observed in the PRD region (8%−28%, Kuang et al., 2015). The intensive wood and crop residue burning activities in the Beijing−Tianjin−Hebei region during autumn and winter could emit a large amount of aerosols into the atmosphere (Zhang et al., 2013). Thus, as shown in Figure 4A, the contribution of biomass burning to $HULIS_{WS}$ in the heating season (2.96 μg m^{-3}) was 3.5 times that in the non-heating season (0.84 μg m^{-3}).

A previous study reported that refuse burning may contribute 1%–24% of organic particles in Asia (Simoneit et al., 2004). In this study, waste incineration was found for the first time as an important source of $HULIS_{WS}$ in Beijing, with a considerable and stable contribution to $HULIS_{WS}$ throughout the year (18.7% in the non-heating season and 17.1% in the heating season). According to the China Statistic Yearbook (2013), 6.33 million tons of domestic waste were produced in Beijing during 2012 (National Bureau of Statistics of China, 2013), among which 0.95 million tons were disposed through incineration. Given that nearly 24% of the urban waste was plastic (Wang and Wang, 2013), the incineration of such large amounts of domestic waste may explain the high levels of TPha in Beijing.

Coal has occupied the predominant position in China's energy consumption for a long time (Zhang and Yang, 2013). Therefore, coal combustion is an important source of $PM_{2.5}$ pollution in China, especially in northern Chinese cities. Tan et al. (2016) identified a strong correlation between $HULIS_{WS}$ and Cl^- ($R^2 = 0.89$) in Lanzhou and suggested that coal burning was probably the major contributor to $HULIS_{WS}$ in winter. However, the contribution of coal combustion to $HULIS_{WS}$ was found to be minor (5.8%) in the present study. Similarly, a source apportionment analysis of $PM_{2.5}$-bound water-soluble organic carbon (WSOC) in Beijing found that less than 5% of WSOC was from coal combustion (Tao et al., 2016). This was because less oxidized compounds including PAHs were favourably produced from the aromatic fragments of coal under the fuel-rich incomplete combustion conditions; these less oxidized compounds are generally hydrophobic substances and not extracted into the $HULIS_{WS}$ fraction.

A correlation between $HULIS_{WS}$ and hopanes ($R^2 = 0.46$, Figure S5 in the Supplementary Material) might suggest direct emissions of $HULIS_{WS}$ from vehicle exhaust. As shown in Figure 4A, vehicle emissions are responsible for 13.7% of $PM_{2.5}$-bound $HULIS_{WS}$. Interestingly, the amount of $HULIS_{WS}$ assigned to vehicle exhaust was approximately three times higher in the heating season than in the non-heating season (Figure 4A). This could be attributed to the low temperature in winter, which favours the partition of semivolatile $HULIS_{WS}$ species into particle phases. Another explanation could be that more $HULIS_{WS}$ were formed from the aging process of traffic exhaust in the heating season. To evaluate this hypothesis, multilinear regression (MLR) analysis was conducted to assess the effects of NO_X, O_3, SO_4^{2-}, particle acidity (H_p^+), and particle-phase liquid water content (LWC_p) on $HULIS_{WS}$ resolved in the vehicle emissions factor ($HULIS_{WS\_VE}$; the calculation of H_p^+ and LWC_p, and the MLR analysis results are provided in the Supplementary Material). NO_X was found as the only statistically significant factor that was positively correlated to $HULIS_{WS\_VE}$ with a regression coefficient of 0.012 ($p < 0.01$; Table S3 in the Supplementary Material), suggesting that a 1 μg m^{-3} increase in NO_X was associated with a 0.012 μg m^{-3} increase in $HULIS_{WS\_VE}$, when holding other covariates unchanged. In fact, vehicle exhaust was the major source of ground level NO_X (>60%) in Beijing, even in the heating season (Lin et al., 2011). A higher level of NO_X was observed during the heating season than during the non-heating season due to a lower boundary layer and weaker vertical mixing (Figure S6 in the Supplementary Material). Kautzman et al. (2010) found that ring-opening oxygenated products with one benzyl group, which could be retained by the HLB cartridge and were considered as $HULIS_{WS}$ components, were predominantly formed from the photo-oxidation of PAHs under high NO_X conditions. Thus, the higher levels of NO_X in the heating season led to higher levels of secondarily produced $HULIS_{WS\_VE}$, indicating a synergistic effect of primary emission and the secondary aging process from vehicle exhaust. Furthermore, the presence of 4M5NC and 3M6NC, SOA markers of cresol, in this factor confirmed that a certain fraction of $HULIS_{WS\_VE}$ was secondarily formed.

In addition to the four combustion-related sources, one secondary source was apportioned by PMF, contributing 30.1% of $HULIS_{WS}$ throughout the year. MLR analysis was conducted to evaluate the effects of O_3, NO_X, SO_4^{2-}, H_p^+, and LWC_p on the secondary formation of $HULIS_{WS}$ ($HULIS_{WS\text{-}SEC}$). Sulfate was found to be the most significant factor with a regression coefficient of 0.066 (Table S4 in the Supplementary Material). This may be due to the predominant role of sulfate in the particle-phase formation of organosulfates, one important $HULIS_{WS}$ component (Xu et al., 2015), through both nucleophilic addition reactions

and the salting-in effect (Lin et al., 2012; Riva et al., 2015). Results from the MLR analysis also indicated that an increase of 1 μg m^{-3} O_3 led to an increase of 0.028 μg m^{-3} $HULIS_{WS\_SEC}$. Gaseous highly oxidized multifunctional organic compounds (HOMs) were characterized in the ozonolysis of α-pinene in smog chamber experiments (Zhang et al., 2015). It was suggested that, after partitioning to the particle phase, these HOMs could undergo rapid accretion reactions to form oligomers containing multiple carboxylic acid and ester groups, which served as good $HULIS_{WS}$ candidates. Considering the higher concentrations of O_3 in the non-heating season (Figure S7 in the Supplementary Material), together with higher biogenic VOCs emissions and temperature as well as more intense solar radiation, a larger amount of $HULIS_{WS\_SEC}$ was produced in the non-heating season (2.01 μg m^{-3}) than in the heating season (1.41 μg m^{-3}).

3.5 Source-specific contributions to DTT activity of $HULIS_{WS}$

To gain quantitative insights into the potential health impacts of different $HULIS_{WS}$ sources, source-specific contributions to extrinsic DTT activity of $HULIS_{WS}$ were assessed using PMF. The strong correlation (R^2 = 0.78; Figure S4 in the Supplementary Material) between measured and predicted DTT activity suggested reliable predictions.

As shown in Figure 4B, the four combustion-related sources accounted for 75% of the extrinsic DTT activity of $HULIS_{WS}$ throughout the year, of which biomass burning contributed 33.6%, followed by vehicle emissions (18.5%), waste incineration (18.5%), and coal combustion (4.1%). The extrinsic DTT activity of $HULIS_{WS}$ describes the redox activity of $HULIS_{WS}$ on air volume basis (E.q.(1)), which is reflective of human exposure to $HULIS_{WS}$; while the intrinsic DTT activities of $HULIS_{WS}$ is on mass basis and is more important for assessing the intrinsic toxicity $HULIS_{WS}$ from various sources. The intrinsic DTT activities of the $HULIS_{WS}$ from the five identified sources were calculated (E.q.(2)). $HULIS_{WS}$ from vehicle emissions was found to be the most DTT-active (12.0 pmol min^{-1} per μg $HULIS_{WS\_VE}$), followed by waste incineration (9.25 pmol min^{-1} per μg $HULIS_{WS\_WI}$), biomass burning (9.10 pmol min^{-1} per μg $HULIS_{WS\_BB}$), secondary formation (7.45 pmol min^{-1} per μg $HULIS_{WS\_SEC}$), and coal combustion (6.22 pmol min^{-1} per μg $HULIS_{WS\_CC}$).

Similar to the source apportionment results of $HULIS_{WS}$, biomass burning was identified as the leading contributor to extrinsic DTT activity of $HULIS_{WS}$ in the heating season (39.4%, 0.015 nmol min^{-1} m^{-3}), and throughout the year (33.6%, 0.017 nmol min^{-1} m^{-3}). During biomass burning, highly oxidized organic compounds with quinone, hydroxyl, and carboxyl groups were directly produced (Fan et al., 2016). Moreover, some of the VOCs emitted from biomass burning could undergo further reactions and generate highly redox-active products, for example, hydroxyquinones formed through ●OH radical oxidation (McWhinney et al., 2013), which could be extracted into the $HULIS_{WS}$ fraction and lead to DTT consumption (Chung et al., 2006; Verma et al., 2015a). Moreover, Wang et al. (2017) found large amounts of nitrogen-containing organic compounds (NOCs) including nitroaromatics and nitrogen-containing bases in $HULIS_{WS}$ from biomass burning. The nitrite group next to aromatic ring in the nitroaromatics could promote electron transfer and lead to more DTT consumption and the nitrogen-containing bases emitted from biomass burning could also enhance the ROS-generation ability of $HULIS_{WS\_BB}$ (Dou et al., 2015), which may explain the observed intrinsic DTT activity of $HULIS_{WS\_BB}$.

Secondary formation was the most important source for the extrinsic DTT activity of $HULIS_{WS}$ in the non-heating season (44.1%, 0.015 nmol min^{-1} m^{-3}) and the second largest contributor throughout the year (25.3%, 0.013 nmol min^{-1} m^{-3}). A few smog chamber experiments have been carried out to investigate the ROS activity of SOA from various hydrocarbon precursors, and the intrinsic DTT activity values of several biogenic SOA systems (i.e. isoprene, α-pinene, and β-caryophyllene) were found to be within the range of 2 to 30 pmol min^{-1} per μg SOA (Kramer et al., 2016; Tuet et al., 2017). Tuet et al. (2017) also observed a much higher intrinsic DTT activity of naphthalene SOA than that of biogenic SOA, and suggested that this was probably due to the aromatic species, especially nitroaromatics, in naphthalene SOA. The intrinsic DTT activity of $HULIS_{WS\_SEC}$ measured in this study is 7.45

pmol min^{-1} per μg $HULIS_{WS\_SEC}$, which is within the reported intrinsic DTT activity range of biogenic SOA. Moreover, results from MLR analysis indicated that both sulfate and ozone were positively correlated with $HULIS_{WS\_SEC}$ (Table S4), suggesting that $HULIS_{WS}$ resolved in this factor could mainly consist of some less ROS-active SOA components, such as organosulfates (Chen et al., 2011; Lin et al., 2012). Although chamber experiments reported the formation of ROS-active HOMs or organic peroxides through the ozonolysis of biogenic VOCs (Docherty et al., 2005; Zhang et al., 2015), the production yields of these peroxides were generally low and thus could not have a major influence on the DTT activity of $HULIS_{WS\_SEC}$. However, since secondary formation predominated in $HULIS_{WS}$ formation (Figure 4A), especially in the non-heating season (50.1%), even with a lower intrinsic DTT activity, secondary aerosol formation still serves as a significant contributor to $HULIS_{WS}$-associated redox activity in Beijing. It should be noted that the contributions of secondary formation processes to both $HULIS_{WS}$ and DTT activity of $HULIS_{WS}$ could even have been underestimated in this study, because $HULIS_{WS}$ secondarily formed through the aging of biomass burning and vehicle emissions was resolved in factor B and D and could not be accurately quantified.

Although vehicle emission just contributed 18% to extrinsic DTT activity of $HULIS_{WS}$ throughout the year (18.5%, 0.009 nmol min^{-1} m^{-3}), $HULIS_{WS\_VE}$ has the highest intrinsic DTT activity among all sources (12.0 pmol min^{-1} per μg $HULIS_{WS\_VE}$). Similarly, Bates et al. (2015) revealed that the water-soluble $PM_{2.5}$ from gasoline vehicle emissions had the highest intrinsic DTT activity, probably due to the oxygenated OC and metals on gasoline particles. Verma et al. (2009) also observed a higher aerosol oxidative potential from the aged particles of traffic exhaust than those directly emitted, and a strong correlation was observed between oxygenated organic acids and vehicle-related redox activity. As shown in Figure 2D, most of the two methyl nitrocatechol markers were resolved in the vehicle emissions factor and $HULIS_{WS\_VE}$ was found to be significantly correlated with NO_X, therefore the high intrinsic ROS activity of $HULIS_{WS\_VE}$ is believed to be mostly due to the highly oxygenated OC content, especially the highly redox-active nitroaromatics (Tuet et al., 2017).

Waste incineration was also an important primary source of the extrinsic DTT activity of $HULIS_{WS}$ (20.5% in the non-heating season and 17.4% in the heating season), and its intrinsic $HULIS_{WS}$ ROS activity was slightly higher than that from biomass burning. Mohr et al. (2009) examined the elemental ratio of aerosols emitted from different sources. They found that particles from plastic burning had a higher O/C ratio (0.08) than those from diesel (0.03) and gasoline (0.04) combustion, indicating a more oxidized feature of aerosols emitted through refuse burning (Mohr et al., 2009). Considering that incineration will play an increasingly important role in waste treatment in Beijing in the following years (National Development and Reform Comission, 2016), concern should be directed to the potential threat of trash burning to public health.

In summary, four combustion-related sources and one secondary formation source of $PM_{2.5}$-bound $HULIS_{WS}$ and their associated ROS activity were identified by PMF. Biomass burning (32.7%) and secondary aerosol formation (30.1%) were the major contributors to $HULIS_{WS}$ in Beijing. For the first time, waste incineration was identified as an important source of $HULIS_{WS}$, with a considerable and stable contribution to $HULIS_{WS}$ throughout the year (17.7%). Regarding ROS-generation potential, $HULIS_{WS}$ from vehicle emissions was identified as the most ROS-active, and $HULIS_{WS}$ from secondary aerosol formation showed a lower intrinsic DTT ability than those of most primary sources except for coal combustion. Such variations in the ROS-generation ability of $HULIS_{WS}$ from different sources will be relevant for future inquiries into more detailed chemical speciation of $HULIS_{WS}$, their roles in ROS generation, and the possible oxidation mechanisms involved.

Supplementary Material. Information on chemical analysis; PMF source apportionment; MLR analysis together with Table S1-S4 and Figure S1-S7 are provided.

Acknowledgement. This work was supported by the National Natural Science Foundation of China (NSFC21477102, 21322705

and 41421064), the Joint NSFC-ISF Research Program (41561144007), the General Research Fund of Hong Kong Research Grant Council (12304215, 12300914 and 201212), the Ministry of Science and Technology of China Grants (973 program; 2015CB553401), the Faculty Research Grant from Hong Kong Baptist University (FRG2/16-17/041), and Research and Development of Science and Technology in Shenzhen (JCYJ 20140419130357038 and JCYJ 20150625142543472). The author would like to thank Binyu Kuang from Hong Kong University of Science and Technology for $HULIS_{WS}$ quantification.

References

Bates, J. T., Weber, R. J., Abrams, J., Verma, V., Fang, T., Klein, M., Strickland, M. J., Sarnat, S. E., Chang, H. H., Mulholland, J. A., Tolbert, P. E. and Russell, A. G.: Reactive oxygen species generation linked to sources of atmospheric particulate matter and cardiorespiratory effects, Environ. Sci. Technol., 49(22), 13605–13612, 2015.

Becker, S., Dailey, L. A., Soukup, J. M., Grambow, S. C., Devlin, R. B. and Huang, Y. C. T.: Seasonal variations in air pollution particle-induced inflammatory mediator release and oxidative stress, Environ. Health Perspect., 113(8), 1032–1038, 2005.

Charrier, J. G. and Anastasio, C.: On dithiothreitol (DTT) as a measure of oxidative potential for ambient particles: Evidence for the importance of soluble transition metals, Atmos. Chem. Phys., 12(19), 9321–9333, 2012.

Chen, X., Hopke, P. K. and Carter, W. P. L.: Secondary organic aerosol from Oozonolysis of biogenic volatile organic compounds : Chamber studies of particle and reactive oxygen species formation, Environ. Sci. Technol., 45(1), 276–282, 2011.

Cheng, C., Wang, G., Zhou, B., Meng, J., Li, J., Cao, J. and Xiao, S.: Comparison of dicarboxylic acids and related compounds in aerosol samples collected in Xi'an, China during haze and clean periods, Atmos. Environ., 81, 443–449, 2013.

Chung, M. Y., Lazaro, R. A., Lim, D., Jackson, J., Lyon, J., Rendulic, D. and Hasson, A. S.: Aerosol-borne quinones and reactive oxygen species generation by particulate matter extracts, Environ. Sci. Technol., 40(16), 4880–4886, 2006.

Docherty, K. S., Wu, W., Lim, Y. Bin and Ziemann, P. J.: Contributions of organic peroxides to secondary aerosol formed from reactions of monoterpenes with O_3, Environ. Sci. Technol., 39(11), 4049–4059, 2005.

Dou, J., Lin, P., Kuang, B. and Yu, J. Z.: Reactive oxygen species production mediated by humic-like substances in atmospheric aerosols: Enhancement effects by pyridine, imidazole, and their Derivatives, Environ. Sci. Technol., 49(11), 6457–6465, 2015.

Fan, X., Wei, S., Zhu, M., Song, J. and Peng, P.: Comprehensive characterization of humic-like substances in smoke $PM_{2.5}$ emitted from the combustion of biomass materials and fossil fuels, Atmos. Chem. Phys., 16(20), 13321–13340, 2016.

Graber, E. R. and Rudich, Y.: Atmospheric HULIS: how humic-like are they? A comprehensive and critical review, Atmos. Chem. Phys., 5(5), 9801–9860, 2006.

Guo, S., Hu, M., Guo, Q., Zhang, X., Zheng, M., Zheng, J., Chang, C. C., Schauer, J. J. and Zhang, R.: Primary sources and secondary formation of organic aerosols in Beijing, China., Environ. Sci. Technol., 46(18), 9846–53, 2012.

Henry, R. C., Lewis, C. W., Hopke, P. K. and Williamson, H. J.: Review of receptor model fundamentals, Atmos. Environ., 18(8), 1507–1515, 1984.

Ho, K. F., Ho, S. S. H., Lee, S. C., Kawamura, K., Zou, S. C., Cao, J. J. and Xu, H. M.: Summer and winter variations of dicarboxylic acids, fatty acids and benzoic acid in $PM_{2.5}$ in Pearl Delta River Region, China, Atmos. Chem. Phys., 11(5), 2197–2208, 2011.

Ho, S. S. H. and Yu, J. Z.: In-injection port thermal desorption and subsequent gas chromatography-mass spectrometric analysis of polycyclic aromatic hydrocarbons and n-alkanes in atmospheric aerosol samples, J. Chromatogr. A, 1059(1–2), 121–129, 2004.

Hu, D., Bian, Q., Li, T. W. Y., Lau, A. K. H. and Yu, J. Z.: Contributions of isoprene, monoterpenes, β-caryophyllene, and toluene to secondary organic aerosols in Hong Kong during the summer of 2006, J. Geophys. Res. Atmos., 113(22), D22206, 2008.

Hu, D., Bian, Q., Lau, A. K. H. and Yu, J. Z.: Source apportioning of primary and secondary organic carbon in summer $PM_{2.5}$ in

Hong Kong using positive matrix factorization of secondary and primary organic tracer data, J. Geophys. Res. Atmos., 115(16), 1–14, 2010.

Huang, C., Wang, H. L., Li, L., Wang, Q., Lu, Q., De Gouw, J. A., Zhou, M., Jing, S. A., Lu, J. and Chen, C. H.: VOC species and emission inventory from vehicles and their SOA formation potentials estimation in Shanghai, China, Atmos. Chem. Phys., 15(19), 11081–11096, 2015.

Iinuma, Y., Böge, O. and Herrmann, H.: Methyl-nitrocatechols: Atmospheric tracer compounds for biomass burning secondary organic aerosols, Environ. Sci. Technol., 44(22), 8453–8459, 2010.

Kahnt, A., Behrouzi, S., Vermeylen, R., Safi Shalamzari, M., Vercauteren, J., Roekens, E., Claeys, M. and Maenhaut, W.: One-year study of nitro-organic compounds and their relation to wood burning in PM_{10} aerosol from a rural site in Belgium, Atmos. Environ., 81, 561–568, 2013.

Kautzman, K. E., Surratt, J. D., Chan, M. N., Chan, A. W. H., Hersey, S. P., Chhabra, P. S., Dalleska, N. F., Wennberg, P. O., Flagan, R. C. and Seinfeld, J. H.: Chemical composition of gas- and aerosol-phase products from the photooxidation of naphthalene, J. Phys. Chem. A, 114(2), 913–934, 2010.

Kawamura, K. and Pavuluri, C. M.: New Directions: Need for better understanding of plastic waste burning as inferred from high abundance of terephthalic acid in South Asian aerosols, Atmos. Environ., 44(39), 5320–5321, 2010.

Kramer, A. J., Rattanavaraha, W., Zhang, Z., Gold, A., Surratt, J. D. and Lin, Y. H.: Assessing the oxidative potential of isoprene-derived epoxides and secondary organic aerosol, Atmos. Environ., 130, 211–218, 2016.

Kuang, B. Y., Lin, P., Huang, X. H. H. and Yu, J. Z.: Sources of humic-like substances in the Pearl River Delta, China: Positive matrix factorization analysis of $PM_{2.5}$ major components and source markers, Atmos. Chem. Phys., 15(4), 1995–2008, 2015.

Li, J., Du, H., Wang, Z., Sun, Y., Yang, W., Li, J., Tang, X. and Fu, P.: Rapid formation of a severe regional winter haze episode over a mega-city cluster on the North China Plain, Environ. Pollut., 1–11, 2017.

Li, Q., Wyatt, A. and Kamens, R. M.: Oxidant generation and toxicity enhancement of aged-diesel exhaust, Atmos. Environ., 43(5), 1037–1042, 2009.

Lin, P. and Yu, J. Z.: Generation of reactive oxygen species mediated by humic-like substances in atmospheric aerosols, Environ. Sci. Technol., 45(24), 10362–10368, 2011.

Lin, P., Huang, X. F., He, L. Y. and Zhen Yu, J.: Abundance and size distribution of HULIS in ambient aerosols at a rural site in South China, J. Aerosol Sci., 41(1), 74–87, 2010a.

Lin, P., Engling, G. and Yu, J. Z.: Humic-like substances in fresh emissions of rice straw burning and in ambient aerosols in the Pearl River Delta Region, China, Atmos. Chem. Phys., 10(14), 6487–6500, 2010b.

Lin, P., Yu, J. Z., Engling, G. and Kalberer, M.: Organosulfates in humic-like substance fraction isolated from aerosols at seven locations in East Asia: A study by ultra-high-resolution mass spectrometry, Environ. Sci. Technol., 46(24), 13118–13127, 2012.

Lin, W., Xu, X., Ge, B. and Liu, X.: Gaseous pollutants in Beijing urban area during the heating period 2007-2008: Variability, sources, meteorological, and chemical impacts, Atmos. Chem. Phys., 11(15), 8157–8170, 2011.

Ma, Y., Cheng, Y., Qiu, X., Lin, Y., Cao, J. and Hu, D.: A quantitative assessment of source contributions to fine particulate matter ($PM_{2.5}$)-bound polycyclic aromatic hydrocarbons (PAHs) and their nitrated and hydroxylated derivatives in Hong Kong, Environ. Pollut., 219, 742-749, 2016.

McWhinney, R. D., Zhou, S. and Abbatt, J. P. D.: Naphthalene SOA: Redox activity and naphthoquinone gas-particle partitioning, Atmos. Chem. Phys., 13(19), 9731–9744, 2013.

Mohr, C., Huffman, J. A., Cubison, M. J., Aiken, A. C., Docherty, K. S., Kimmel, J. R., Ulbrich, I. M., Hannigan, M. and Jimenez, J. L.: Characterization of primary organic aerosol emissions from meat cooking, trash burning, and motor vehicles with high-

resolution aerosol mass spectrometry and comparison with ambient and chamber observations, Environ. Sci. Technol., 43(7), 2443–2449, 2009.

National Bureau of Statistics of China: China Statistic Yearbook (2013), 2013.

National Development and Reform Comission: National urban waste harmless treatment facilities' construction for the 13th five years., 2016.

Nel, A.: Air pollution – related Illness : Effects of particles, Science, 308(5723), 804–806, 2005.

Norris, G., Duvall, R., Brown, S. and Bai, S.: EPA positive matrix factorization (PMF) 5.0 fundamentals and user guide, U.S. Environmental Protection Agency., 2014.

Riva, M., Tomaz, S., Cui, T., Lin, Y. H., Perraudin, E., Gold, A., Stone, E. A., Villenave, E., Surratt, J. D., Toma, S., Cui, T., Lin, Y. H. and Perraudin, E.: Evidence for an unrecognized secondary anthropogenic source of organosulfates and sulfonates: Gas-phase oxidation of polycyclic aromatic hydrocarbons in the presence of sulfate aerosol, Environ. Sci. Technol., 49(11), 6654–6664, 2015.

Sato, K., Takami, A., Kato, Y., Seta, T., Fujitani, Y., Hikida, T., Shimono, A. and Imamura, T.: AMS and LC/MS analyses of SOA from the photooxidation of benzene and 1,3,5-trimethylbenzene in the presence of NOx: Effects of chemical structure on SOA aging, Atmos. Chem. Phys., 12(10), 4667–4682, 2012.

Simoneit, B. R. T., Kobayashi, M., Mochida, M., Kawamura, K., Lee, M., Lim, H. J., Turpin, B. J. and Komazaki, Y.: Composition and major sources of organic compounds of aerosol particulate matter sampled during the ACE-Asia campaign, J. Geophys. Res. D Atmos., 109(19), 1–22, 2004.

Simoneit, B. R. T., Medeiros, P. M. and Didyk, B. M.: Combustion products of plastics as indicators for refuse burning in the atmosphere, Environ. Sci. Technol., 39(18), 6961–6970, 2005.

Tan, J., Xiang, P., Zhou, X., Duan, J., Ma, Y., He, K., Cheng, Y., Yu, J. and Querol, X.: Chemical characterization of humic-like substances (HULIS) in $PM_{2.5}$ in Lanzhou, China, Sci. Total Environ., 573, 1481–1490, 2016.

Tang, Q., Hu, M., Wang, Z. and Kuang, B.: Chemical composition of fine and coarse particles at Wuqing during the HaChi summer campaign, in The 7 th Asian Aerosol Conference, p.322., 2011.

Tao, J., Zhang, L., Zhang, R., Wu, Y., Zhang, Z., Zhang, X., Tang, Y., Cao, J. and Zhang, Y.: Uncertainty assessment of source attribution of $PM_{2.5}$ and its water-soluble organic carbon content using different biomass burning tracers in positive matrix factorization analysis - a case study in Beijing, China, Sci. Total Environ., 543(7), 326–335, 2016.

Tuet, W. Y., Chen, Y., Xu, L., Fok, S., Gao, D., Weber, R. J. and Ng, N. L.: Chemical oxidative potential of secondary organic aerosol (SOA) generated from the photooxidation of biogenic and anthropogenic volatile organic compounds, Atmos. Chem. Phys., 17(2), 839–853, 2017.

Verma, V., Ning, Z., Cho, A. K., Schauer, J. J., Shafer, M. M. and Sioutas, C.: Redox activity of urban quasi-ultrafine particles from primary and secondary sources, Atmos. Environ., 43(40), 6360–6368, 2009.

Verma, V., Fang, T., Guo, H., King, L., Bates, J. T., Peltier, R. E., Edgerton, E., Russell, A. G. and Weber, R. J.: Reactive oxygen species associated with water-soluble $PM_{2.5}$ in the southeastern United States: Spatiotemporal trends and source apportionment, Atmos. Chem. Phys., 14(23), 12915–12930, 2014.

Verma, V., Wang, Y., El-Afifi, R., Fang, T., Rowland, J., Russell, A. G. and Weber, R. J.: Fractionating ambient humic-like substances (HULIS) for their reactive oxygen species activity - Assessing the importance of quinones and atmospheric aging, Atmos. Environ., 120, 351–359, 2015a.

Verma, V., Fang, T., Xu, L., Peltier, R. E., Russell, A. G., Ng, N. L. and Weber, R. J.: Organic aerosols associated with the generation of reactive oxygen species (ROS) by water-soluble $PM_{2.5}$, Environ. Sci. Technol., 49, 4646–4656, 2015b.

Wang, H. and Wang, C.: Municipal solid waste management in Beijing: characteristics and challenges., Waste Manag. Res., 31(1), 67–72, 2013.

Wang, H. and Wang, C.: Municipal solid waste management in Beijing: characteristics and challenges., Waste Manag. Res., 31(1), 67–72, 2013.

Wang, Y., Hu, M., Lin, P., Guo, Q., Wu, Z., Li, M., Zeng, L., Song, Y., Zeng, L., Wu, Y., Guo, S., Huang, X. and He, L.: Molecular characterization of nitrogen-containing organic compounds in humic-like substances emitted from straw residue burning, Environ. Sci. Technol., 51(11), 5951–5961, 2017.

Xing, L., Fu, T. M., Cao, J. J., Lee, S. C., Wang, G. H., Ho, K. F., Cheng, M. C., You, C. F. and Wang, T. J.: Seasonal and spatial variability of the OM/OC mass ratios and high regional correlation between oxalic acid and zinc in Chinese urban organic aerosols, Atmos. Chem. Phys., 13(8), 4307–4318, 2013.Xu, L., Guo, H., Boyd, C. M., Klein, M., Bougiatioti, A., Cerully, K. M., Hite, J. R., Isaacman-VanWertz, G., Kreisberg, N. M., Knote, C., Olson, K., Koss, A., Goldstein, A. H., Hering, S. V, de Gouw, J., Baumann, K., Lee, S.-H., Nenes, A., Weber, R. J. and Ng, N. L.: Effects of anthropogenic emissions on aerosol formation from isoprene and monoterpenes in the southeastern United States., Proc. Natl. Acad. Sci. U. S. A., 112(1), 37–42, 2015.

Zhang, R., Jing, J., Tao, J., Hsu, S. C., Wang, G., Cao, J., Lee, C. S. L., Zhu, L., Chen, Z., Zhao, Y. and Shen, Z.: Chemical characterization and source apportionment of $PM_{2.5}$ in Beijing: Seasonal perspective, Atmos. Chem. Phys., 13(14), 7053–7074, 2013.

Zhang, W. and Yang, S.: The influence of energy consumption of China on its real GDP from aggregated and disaggregated viewpoints, Energy Policy, 57, 76–81, 2013.

Zhang, X., McVay, R. C., Huang, D. D., Dalleska, N. F., Aumont, B., Flagan, R. C. and Seinfeld, J. H.: Formation and evolution of molecular products in α-pinene secondary organic aerosol, Proc. Natl. Acad. Sci. U. S. A., 112(46), 14168–14173, 2015.

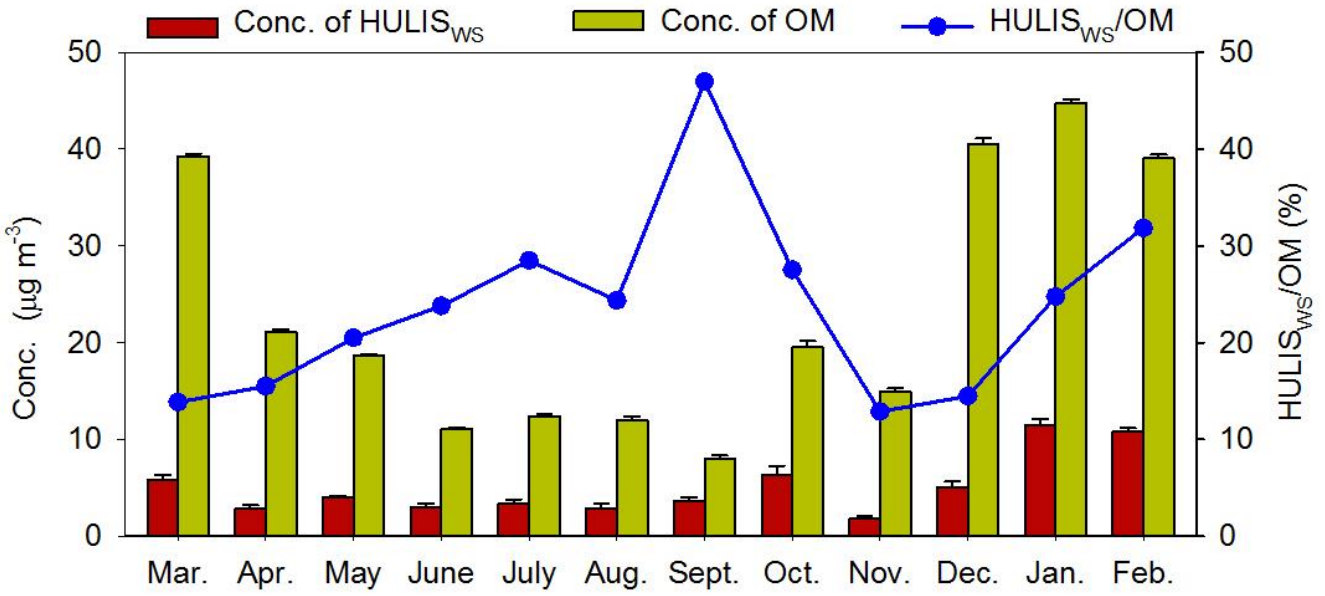

Figure 1: Monthly average concentrations (average ± standard error) of HULIS$_{WS}$ mass concentration and organic matter (OM) in $PM_{2.5}$ collected in Beijing. The monthly percentage contributions of HULIS$_{WS}$ to OM are shown in the blue line.

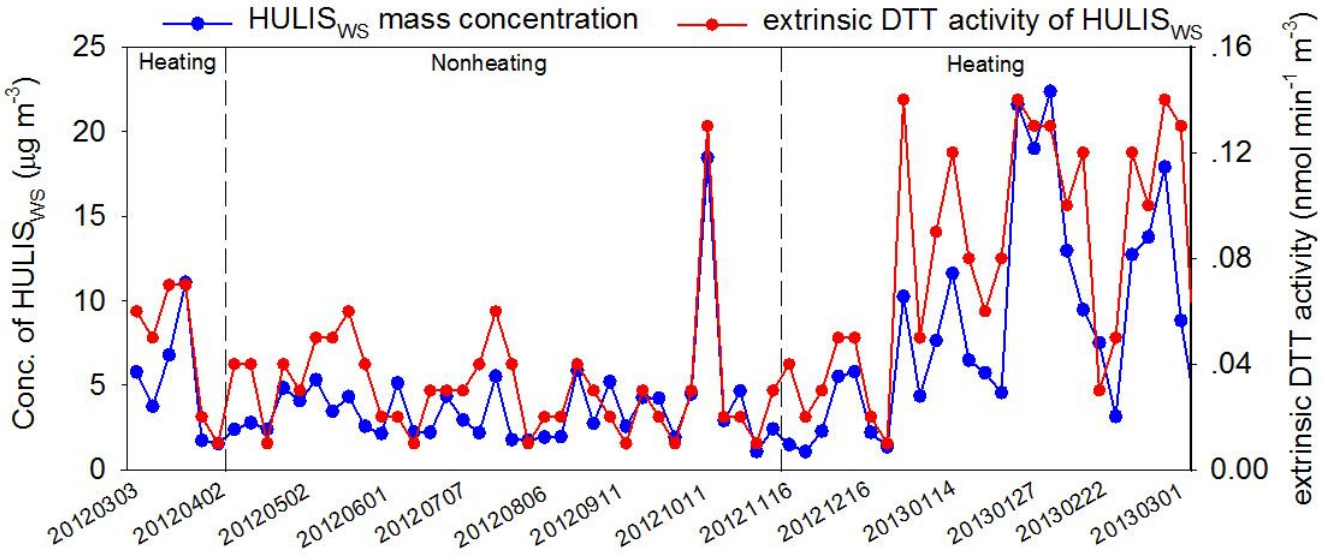

Figure 2: Temporal variation of HULIS$_{WS}$ mass concentration and extrinsic DTT activity of HULIS$_{WS}$ in Beijing.

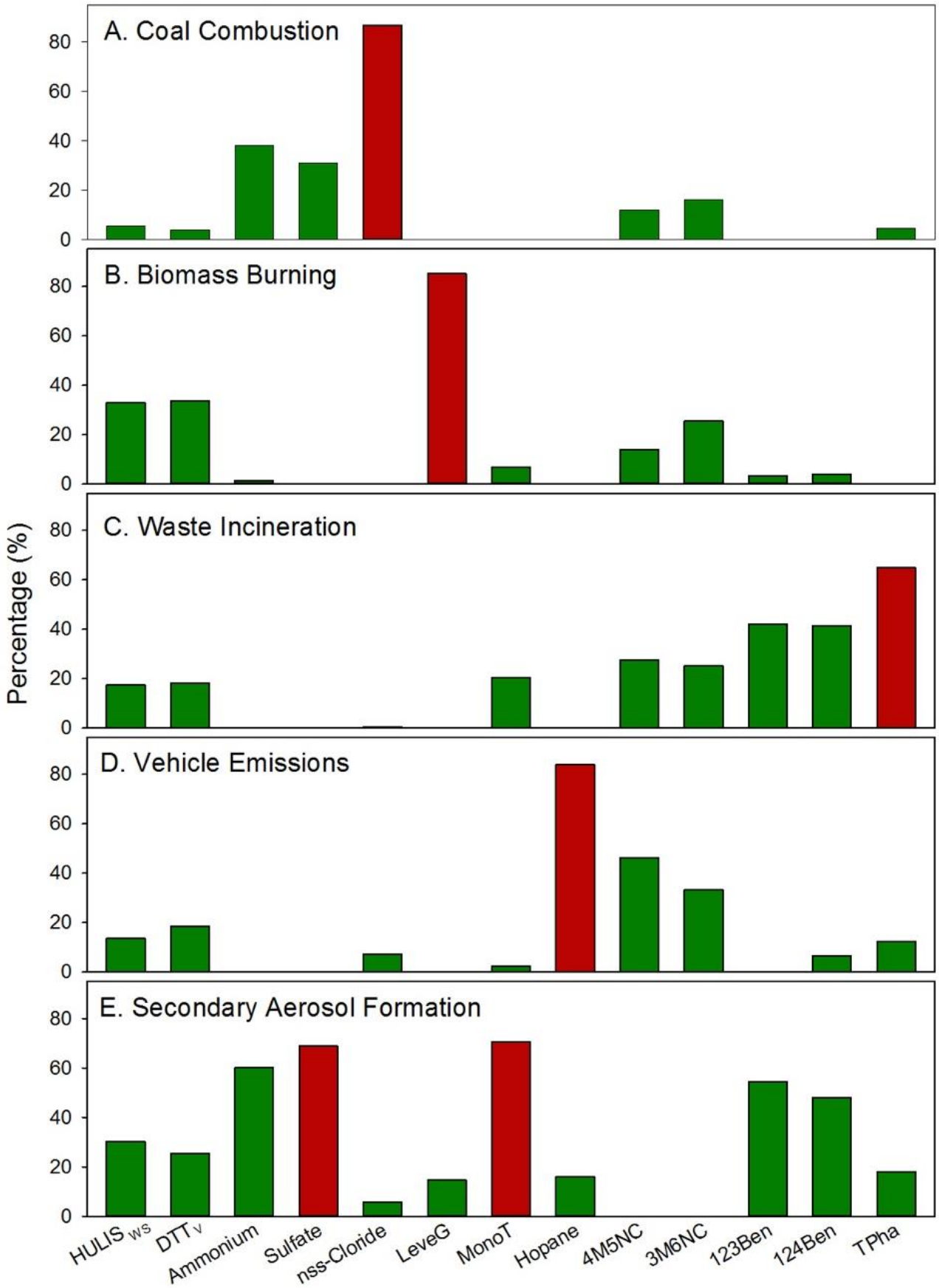

Figure 3: Distribution of HULIS$_{WS}$, HULIS$_{WS}$-associated DTT activity and other measured species in the five sources resolved by PMF. Columns in dark red indicate characteristic tracers of each source.

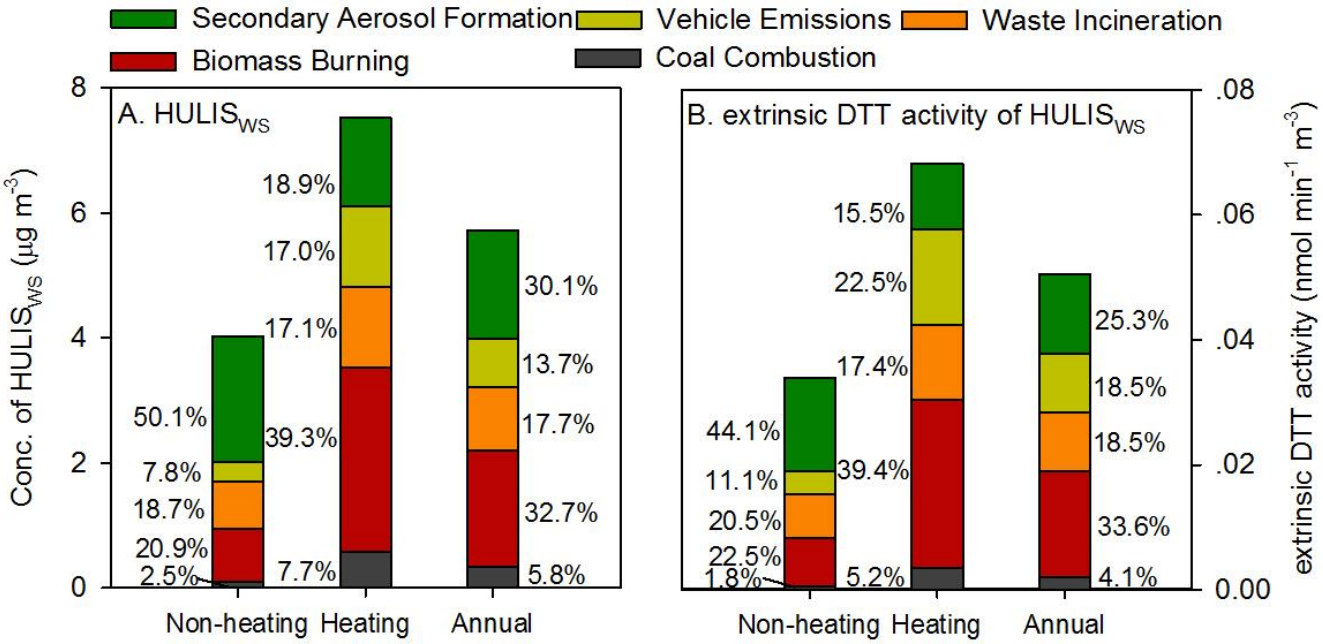

Figure 4: Source-specific contributions to HULIS$_{WS}$ mass concentration (panel A) and extrinsic DTT activity of HULIS$_{WS}$ (panel B).